

FIELD EMISSION FROM SINGLE CRYSTAL AND LARGE GRAIN NIOBIUM CATHODES

Arti Dangwal^{#,a}, Günter Müller, Berg. Universität Wuppertal, D-42097 Wuppertal, Germany
Detlef Reschke, Xenia Singer, ^aDESY, D-22603 Hamburg, Germany

Abstract

Appreciable suppression of field emission from metallic surfaces has been achieved by the use of improved surface cleaning techniques, and dry ice cleaning has emerged recently as a very effective tool in this respect. In order to understand the effects of surface preparation on field emission, systematic measurements were performed on five single crystal and three large grain samples of high purity ($RRR > 300$) Nb by means of AFM, XRD, SEM and dc field emission scanning microscope. The samples were treated with buffered chemical polishing (BCP), half of those for 30 μm and others for 100 μm removal of surface damage layer, followed by a final high pressure water rinsing. The samples with longer BCP treatment showed the onset of field emission at slightly higher fields. A low temperature (~ 150 °C) heat treatment in high vacuum (10^{-6} mbar) chamber for 14 hours, on a selected large grain Nb sample, gives the evidence for the grain boundary assisted FE at very high fields of 250 and 300 MV/m. Finally, an interesting correlation between sizes of all investigated emitters derived from SEM images with respect to their respective onset fields has been found, which might facilitate the quality control of superconducting radio-frequency cavities for linear accelerators.

INTRODUCTION

Highly purified fine grain niobium sheets ($RRR > 250$) have been used worldwide for the fabrication of high gradient superconducting accelerator cavities in various projects like FLASH [1], SNS [2] and RIA [3]. Much attention has been given to the surface preparation and cleanliness techniques, which has suppressed significantly the enhanced field emission (FE) of electrons from the cavity surface and thus improved the regular cavity performance at high accelerating gradients, e.g. up to about $E_{\text{acc}} = 30$ MV/m for nine-cell 1.3 GHz structures [4]. High pressure rinsing (HPR) with ultra pure water is used as standard technique for the final cleaning of such cavities [5], while dry ice cleaning (DIC) has emerged recently to be very effective tool in this respect [6]. The best DIC single crystal Nb sample did not provide any FE up to a electric surface field E_s ($\approx 2E_{\text{acc}}$) of 250 MV/m. Further, the removal of field emitting particulates down to 400 nm size and partial smoothing of edges of the protrusions by DIC of Nb surface was also reported.

An approach towards improving the cavity fabrication for future linear accelerators like XFEL [7] and ILC [8]

has been made by using buffered chemically polished (BCP) large grain Nb (LGNb) or single crystal Nb (SCNb) instead of electropolished (EP) polycrystalline Nb, which might be less expensive due to the elimination of sheet fabrication and related processes. Preliminary tests of single cell cavities made from large grain Nb have yielded E_{acc} up to 45 MV/m, which is one of the highest value achieved yet. [9] Further research on multi-cell structures made from large grain or single crystal Nb is required before it can replace polycrystalline Nb. It has also been reported recently that the grain boundaries on large grain Nb cavities provide some, although not dominant, contribution to the hot spots in corresponding thermal maps. [10] Since grain boundaries get easily contaminated by the segregation of impurities during the usual bakeout of cavities, it is interesting to investigate their role for field emission, too.

In this paper, we report on FE properties and surface characteristics of eight large grain and single crystal samples, measured by means of field emission scanning microscope (FESM) [11], scanning electron microscope (SEM), atomic force microscope (AFM), and X-ray diffraction (XRD). In-situ heat treatments at 150 °C were performed on two samples and then measured again to find any change in corresponding FE properties. Intrinsic FE measurements on such a high quality samples were possible due to their very smooth surfaces and the derived β values for different crystal orientations will also be discussed here. Finally, a correlation between sizes of all investigated emitters derived from SEM images and their respective onset fields will be presented.

SAMPLE PREPARATION AND SURFACE QUALITY CONTROL

Five single crystal and three large grain Nb samples of 28 mm diameter were fabricated at DESY Hamburg. The RRR value of the material was at least 300 with Ta content of ~ 300 ppm. Final surface preparation using BCP in HF(40%):HNO₃:(65%) H₃PO₄ (85%) in volume ratio 1:1:2 at temperature 12-18°C has resulted in a mirror-like surface. For half of the samples a surface damage layer of 30 μm and 100 μm was removed, respectively, with the intention of finding the impact of longer BCP treatment on the FE properties of the sample surface. AFM and XRD measurements were performed by means of instruments "easyScan AFM" (NanoSurf AG) and Philips PW1830. The details of samples with surface preparation, crystal orientations, and roughness are summarized in Tab. 1.

The high resolution optical microscopic images of samples SCNb5 and LGNb3 in Fig 1(a) and (b)

[#]corresponding author: arti@physik.uni-wuppertal.de

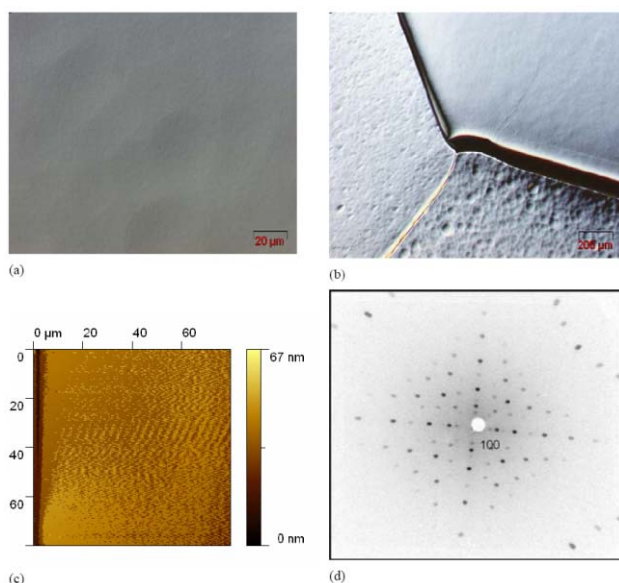


Fig. 1: (a) High resolution optical microscope image of sample SCNb5, (b) microscopic view of intersection of grain boundaries on large grain sample LGNb3, (c) AFM image of sample SCNb5 showing root mean square roughness of 7.5 nm over (80×80) μm² area, and (d) XRD image of SCNb5 revealing (100) orientation.

demonstrate the appearance of different grains of niobium, and the AFM image in Fig 1 (c) provides the surface roughness value of 7.5 nm for Nb(100) oriented surface (Fig. 1 (d)). 100 μm polished single crystal Nb surfaces possess less surface roughness (6-7.2 nm) than 30 μm polished ones (12-17.5 nm), while the large grain samples become as smooth only for 100 μm BCP. All the samples were especially marked during fabrication to adjust the sample position in different experimental setups and were finally rinsed with ultra pure water and HPR.

Table.1: Overview of the investigated single crystal and large grain Nb samples. (nm: not measured samples)

Sample	Removed layer	Orientation	Surface roughness
SCNb1	30μm	(110)	11.7 nm
SCNb2	30μm	(110)	17.6 nm
SCNb3	100 μm	(110)	7.0 nm
SCNb4	100 μm	(111)	6.2 nm
SCNb5	100 μm	(100)	7.5 nm
LGNb1	30μm	(110), (111), (110)	100, 110.5, 62.7
LGNb2	30μm	nm	nm
LGNb3	100 μm	(100), (110), (111)	8.8, 6.9, 6.8

The FE measurements were performed on the flat Nb cathodes under ultrahigh vacuum conditions in FESM,

using conical anodes. The samples were first scanned over a selected area of (12×12) and (10×10) mm² at 90 and 120 MV/m with 300 μm anode and then at 150 and 200 (or 250 and higher) MV/m with 100 μm anode over the areas of (7.5×7.5) and (5×5) mm², respectively. The strong emitters in the observed electric field (E) maps were localized and studied for their individual FE properties. An oven (Kamrath and Weiss) with Pt100 resistor, installed in the high vacuum chamber of FESM, was used to heat the samples at 150 (±10) °C. Efforts were made finally to identify the emitters ex situ in SEM and to reveal their origin from geometrical features and chemical compositions with EDX.

FIELD EMISSION RESULTS AND DISCUSSION

Statistical overview of the emitters

All large grain and single crystal Nb samples have provided very good results, as summarized in Tab. 2. FE maps on large grain Nb samples showed the onset of FE at 120 MV/m for 30 μm and at 150 MV/m for 100 μm polished surfaces. For single crystal Nb sample with 30 and 100 μm BCP, the onset of FE was observed at 150 MV/m and 200 MV/m, respectively. The typical FE maps, given in Fig. 2, show the observed emitters at the highest scanned field levels for these two cases. If we compare the number of emitters at different field levels for all samples from Tab. 2, a marked difference between 30 μm BCP'd LGNb samples (LGNb1 and 2) and all others is observed. It is interesting to discover that it can be directly related to the large difference in the surface roughness values, which is of the order of 100 nm for former and about 10 nm for the later (Tab. 1). Thus, FE was strongly suppressed for smoother surfaces.

Table 2: Emitters observed in FE maps of all Nb samples (see Tab. 1) at different field levels.

Sample	Number of emitters			
	@ 120 MV/m (10mm) ²	@ 150 MV/m (7.5mm) ²	@ 200 MV/m (5mm) ²	@ 250 MV/m (5mm) ²
SCNb1	0	2	5	-
SCNb2	0	1	9	-
SCNb3	0	0	3	9
SCNb4	0	0	2	7
SCNb5	0	0	2	3
LGNb1	2	5	10	-
LGNb2	0	3	12	-
LGNb3	0	1	4	11

A statistical overview of the number density of emitters N for varying electric field E is presented in Fig.3. In order to reduce the statistical error and to simplify the N(E) plot, all the results for a particular kind of samples

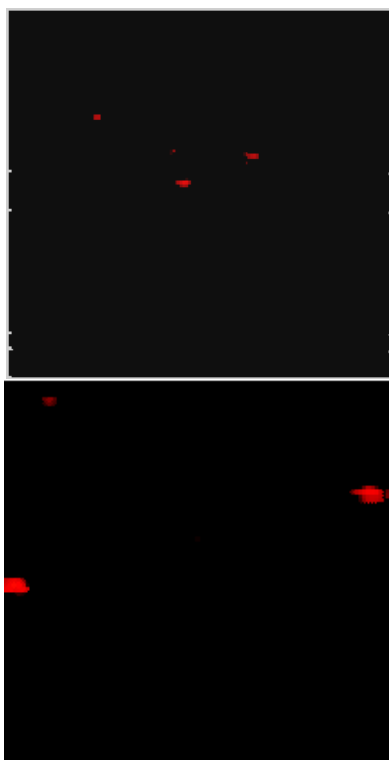


Fig. 2: E-maps for (a) SCNb1 and (b) SCNb5, over the area of (5×5) mm² using a 100 μ m conical anode. The red dots reveal 5 and 3 emitters at onset fields (for 2 nA) of about 200 and 250 MV/m, respectively.

have been summed up, i.e. the corresponding areas and number of emitters were added at the given scanned field levels. Within statistical errors, for LGNb with 30 and 100 μ m BCP, the onset of FE was observed at 120 and 150 MV/m, while for SCNb at 150 and 200 MV/m, respectively. Despite of a significant statistical error, for more damage layer removal there is a tendency of $N(E)$ exponential fit lines to shift to the right, i.e. to higher onset fields and an evidence for reduced slopes, i.e. less number density of field emitters at a given field level. For comparison with the best quality electropolished Nb samples, the corresponding fit line has also been plotted, showing clearly the better performance of SCNb and LGNb samples. These observations are consistent with the earlier findings that the damage layer greater than 50 μ m has to be removed for better cavity performance. [12, 13]

Grain boundary effects and low temperature heat treatment

Present high quality Nb samples should be informative to study any grain boundary effect on FE, due to the presence of either no grain boundary or very few but large grain boundaries easily visible on the sample surface. However, no FE was observed from grain boundaries up to the field of 250 MV/m from any of the as-prepared large grain Nb samples.

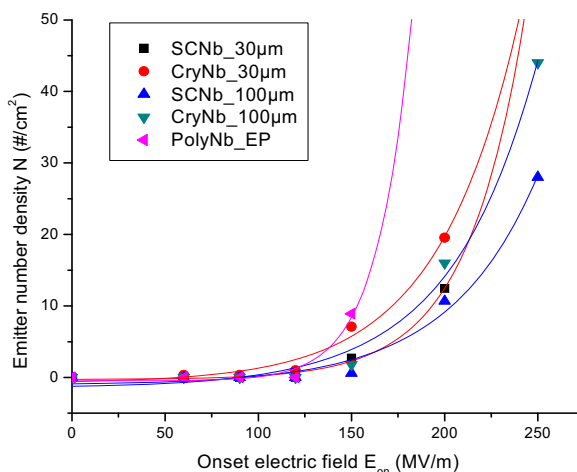


Fig. 3: Emitter number density vs. applied electric field for different damage layer removal. (Exponential fit lines: Red for 30 μ m BCP, blue for 100 μ m BCP, and magenta for EP polycrystalline Nb sample)

Heat treatment (HT) of polycrystalline Nb cavities at low temperatures (100 – 150 °C) is used as a final preparation step, which improves the quality factor of cavities probably by the diffusion of oxygen from surface oxide into the bulk niobium. [14] Analogous to this cavity treatment, we have selected two samples LGNb3 and SCNb4 for low temperature heat treatments at 150°C for 14 and 8 hours, respectively. The corresponding FE maps made after HT are shown in Fig.4. It is interesting to find that on the LGNb sample, most of the emitting sites were activated near or on the grain boundaries, which are 89% at 250 MV/m and 63% at 300 MV/m of total number of emitters. No features in SEM were observed corresponding to these emitters. Two grain boundaries possessing more emitters nearby have the step height of ~12-15 μ m, while the third one has the step height less than 0.5 μ m, as measured by the Profilometer (Fig. 4 (a)). Further it is notable that the strongest emission is observed at the intersection of three grain boundaries. On the other hand, the number of emitters for SCNb remained unchanged up to 200 MV/m as before HT, while at 250 MV/m, one new emitter appeared, and three old emitters disappeared (Fig. 4 (b)). Within statistical error, low temperature HT on SCNb did not show any change on its FE properties. Thus, first evidence for grain boundary assisted FE is observed on LGNb, but only after HT. This is due to easier segregation of impurities along grain boundaries during HT. Our results also show the need of performing similar measurements at higher temperatures for comparison with 800 °C annealing of cavities. More samples measurements are required for a better understanding of grain boundary effects on FE, and should be analyzed with SEM before and after HT.

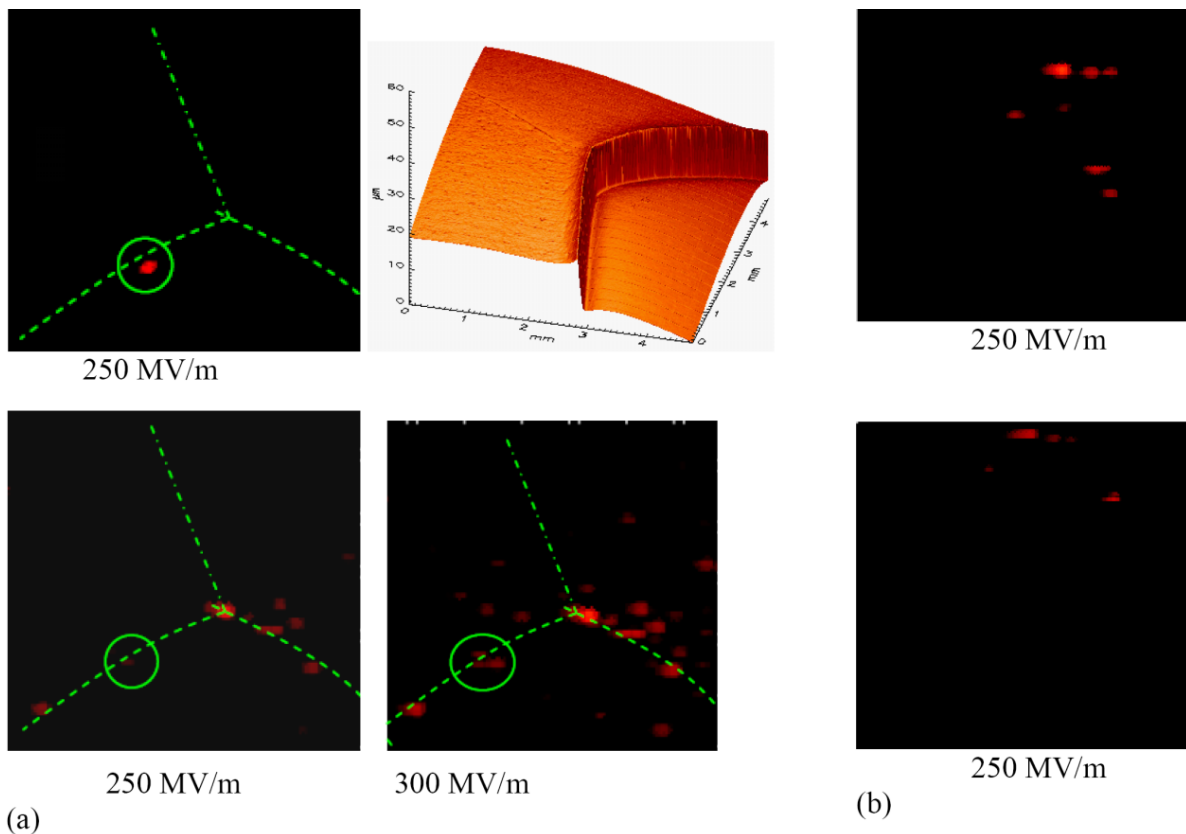


Fig. 4: (a) E-maps of LGNb3, and surface profile (measured with FRT MicroProf®) showing grain boundaries. The encircled emitter is the one activated before HT, and dotted lines in the scan represent the grain boundaries. (b) E-maps for SCNb4: the vertical shift of scans before and after HT is an experimental artifact. All the scans were made on the same area of $(5 \times 5) \text{ mm}^2$ scanned before (upper) and after 150°C heat treatment (lower row) up to the given maximum fields.

Single emitter investigations

The strong emitters appearing in the FE maps of all scanned samples were localized in FESM as well as in SEM (later on) to study their individual FE characteristics with respect to their physical properties. In all cases, the observed emission confirmed FN theory with local field enhancement [15]. Moreover, the phenomenon of activation, deactivation and stabilization of the emitters were generally observed in the continuous up and down cycles of applied electric fields during I-V measurements. The features observed for emitters in SEM investigations, were generally surface irregularities (67%) and particulates (33%) with or without foreign elements present. On $100 \mu\text{m}$ polished samples, presence of a foreign element (aluminium) was detected only in one case (Fig 5 (a)), which might have come from the Al cap used in the transport system of the samples. The corresponding FN curves are changing in different increasing and decreasing modes of electric fields showing the emitters not being stable and might not be properly connected to the surface. The retrieved β value of 26 and S value of $6 \times 10^{-6} \mu\text{m}^2$ seem reasonable for the nm size sharp features present on this flake like object, which might dominate to the local field enhancement.

In the case of heat treated samples, it was interesting to find that the FN curves of all the emitters were rather straight, i.e. showing stable FN behaviour probably due to good contact of emitters with the smooth surface. A typical example is given in Fig. 5 (b). The retrieved β and S values on HT samples were found in the range of (12-57) and $(10^{-3}-10^{-7}) \mu\text{m}^2$, respectively, which are very reasonable for a nanometer to sub-nanometer size effective emission area.

Intrinsic FE measurements

The superior quality of presented single crystal Nb samples makes them suitable for intrinsic FE measurements. These measurements require absolutely clean cathode surface and anode tips, and a very small vacuum gap (down to $2 \mu\text{m}$) for gaining high fields of $\sim 1 \text{ GV/m}$ by means of the 5 KV power supply. Samples SCNb4 of (111) and SCNb7 of (100) orientation were measured in defect free areas with the freshly prepared W anodes of 5-20 μm tip diameter. Since the measurements were very much sensitive to system vibrations, the anode tips as well as the sample surface were often damaged during measurements by microdischarges, (inset of Fig. 6 (a)). The measured FN curves exhibit real FN-like behaviour (Fig. 6), showing the onset of FE at fields higher than 1 GV/m . Assuming β equal to one for our

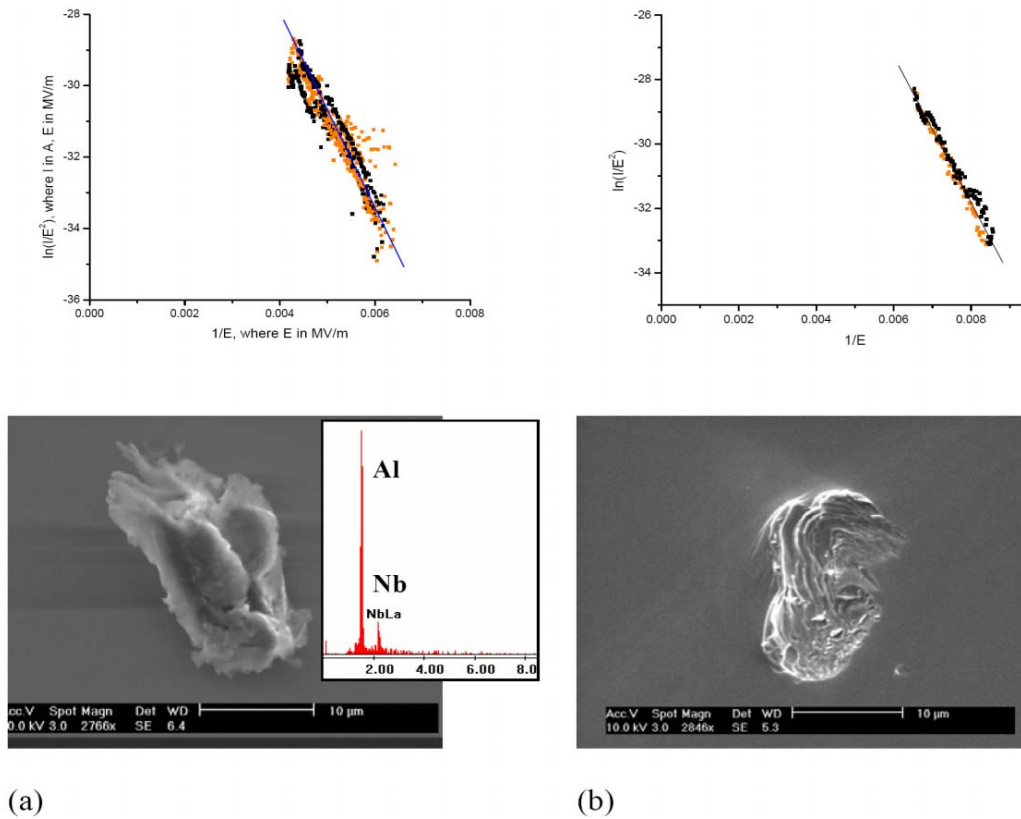


Fig. 5: I-V curves as FN plots of two emitters measured locally in FESM and corresponding SEM images (a) on SCNb7, showing an Al particulate, and (b) on SCNb4, a surface irregularity.

smooth and single crystal samples, we retrieved the β values of Nb with respect to different orientations from FN curves. The fitted mean β values for Nb (111) and Nb (100) are 4.05 and 3.76 within the error of 17 % and 27 %, respectively. These values are in accordance to literature data for the given orientations of Nb. [16, 17] Earlier reported intrinsic measurements on chemically

polished polycrystalline Nb have resulted in β values of about 2 on considering a work function Φ of 4 eV for Nb. [18] On the basis of these results, we conclude that according to the effective protrusion model [19], surface roughness surely enhances the β of particulates and thus the field emission of polycrystalline Nb cavities.

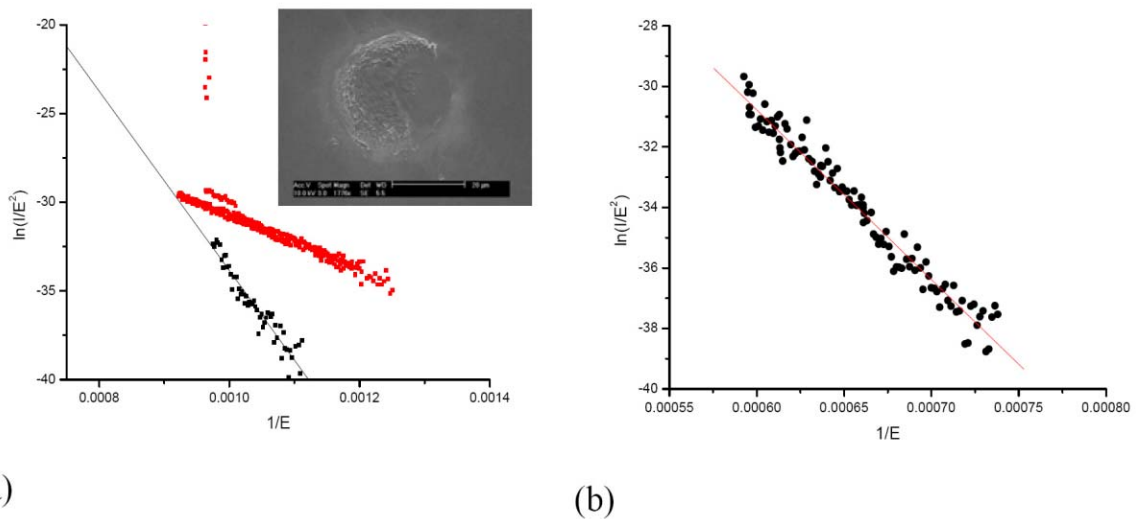


Fig. 6: I-V curves as FN plots locally measured on sample (a) SCNb4, showing the creation of an emitter by a microdischarge with resulting surface damage (inset SEM image) and (b) SCNb7, showing intrinsic field emission of Nb ($\beta = 1$, $\Phi = 4$ eV) .

Emitter size vs. onset electric field (E_{on})

In the last three years, we have measured many samples with different types of Nb surfaces (EP polycrystalline and BCP large grain or single crystal). The analysis of localized emitters in FESM and SEM has resulted in a suggestive plot (Fig. 7) of emitter size derived from SEM images vs. corresponding onset electric fields. Particulate emitters are represented there with their average size and surface irregularities with their widths, because e.g. for a scratch it is the parameter deciding over the height of the edges which causes EFE.

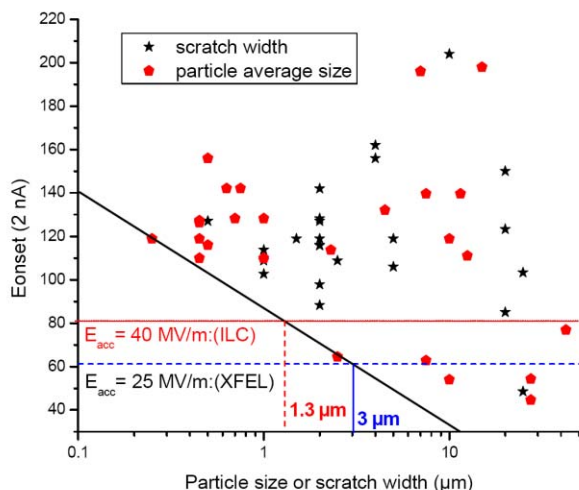


Fig. 7: Onset electric fields for 2 nA FE currents vs. geometrical size of all identified emitters found on various Nb samples during the last 3 years. The horizontal lines correspond to the proposed accelerating fields for future accelerators XFEL and ILC, and the diagonal line sets a corresponding threshold for tolerable defect sizes.

A huge spread in the emitter size is observed in the plot. The diagonal line, however, is referred as a threshold for the minimum emitter size and correspondingly achievable onset fields. Accordingly, to achieve an accelerating gradient of 30 (40) MV/m for XFEL (ILC) [7, 8], surface defects larger than 3 (1.3) μm must be avoided. This result will surely be useful for the quality control of superconducting structures during the assembly of large accelerator projects.

CONCLUSIONS

Single crystal and large grain Nb samples treated with BCP/HPR as a final surface preparation step have been found to show no FE up to surface electric fields of 150 MV/m. The onset fields were slightly higher for the samples with 100 μm removed damage layer than those with 30 μm , and also for single crystals compared to large grain samples due to reduced surface roughness. Heat treatment of large grain Nb sample at 150°C for 14 hours has given first evidence for grain boundary assisted field emission. Intrinsic FE measurements revealed anisotropic β values of 4.02 and 3.8 for (111) and (100) orientations

of Nb, respectively. From last three years EFE investigations on different Nb surfaces, a correlation between size of emitters and onset fields is obtained, which sets a threshold for the tolerable defect size to achieve the envisaged accelerating gradients in superconducting cavities reliably.

ACKNOWLEDGMENTS

We would like to acknowledge C. S. Pandey from BUW for the support on the reinstallation of oven in FESM and thank the Electrical Engineering Department at BUW for access to SEM and EDX facilities. Stimulating discussions with W. Singer and D. Proch from DESY are appreciated. The support of the European Community Research Infrastructure Activity under FP6 "Structuring the European Research Area" program (CARE, contract number RII3-CT-2003-506395) is gratefully acknowledged.

REFERENCES

- [1] <http://flash.desy.de>
- [2] <https://neutrons.ornl.gov/>
- [3] <http://www.orau.org/ria/>
- [4] G. Ciovati, Proc. of LINAC 2006, Knoxville, Tennessee USA
- [5] P. Kneisel and B. Lewis, Proc. of 7th Workshop on RF Superconductivity, Gif sur Yvette, France, ed. by B. Bonin, p. 311, (1995).
- [6] A. Dangwal, G. Müller, D. Reschke, K. Floettmann, and X. Singer, J. Appl. Phys. 102, 2007.
- [7] <http://xfel.desy.de>
- [8] <http://www.interactions.org/linearcollider>
- [9] P. Kneisel, G. R. Myneni, G. Ciovati, J. Sekutowicz, and T. Carneiro, Proc. 2005 Part. Acc. Conf., Knoxville, Tennessee, p3991.
- [10] G. Ciovati, P. Kneisel, and A. Gurevich, Phys. Rev. ST Accel. Beams 10, 062002 (2007).
- [11] D. Lysenkov and G. Müller, Int. J. Nanotechnol. 2, 239 (2005).
- [12] E. Mahner et al., Proc. 6th workshop on RF superconductivity, Newport News, Virginia (1993), p.1085.
- [13] P. Kneisel, Jefferson Lab, Newport News, VA 23606.
- [14] B. Visentin, Y. Gasser, and J.P. Charrier, 12th Workshop on RF Superconductivity, Ithaca USA (2005): TUP05.
- [15] R. H. Fowler and L. Nordheim, Proc. R. Soc. London A119, 173 (1928).
- [16] R. Pantel, M. Bujor, and J. Bardolle, Surf. Sci. 62, 589 (1977).
- [17] I. A. Podchernyaeva, G. V. Samsonov, and V. S. Fomenko, p721, translated from Izvestiya Vyssikh Uchebnykh Zavedenii, Fizika 12, pp. 42-47 (1969).
- [18] T. Habermann, PhD thesis, Univ. of Wuppertal (1999).
- [19] M. Jimenez, R. J. Noer, G. Jouve, J. Jodet, and B. Bonin, J. Phys. D: Appl. Phys. 27, 1038 (1994).